BehaviorGPT: Smart Agent Simulation for Autonomous Driving with Next-Patch Prediction

Zikang Zhou[*]
City University of Hong Kong
zikanzhou2-c@my.cityu.edu.hk

Haibo Hu[*]
City University of Hong Kong
haibohu2-c@my.cityu.edu.hk

Xinhong Chen
City University of Hong Kong
xinhong.chen@cityu.edu.hk

Jianping Wang
City University of Hong Kong
jianwang@cityu.edu.hk

Nan Guan
City University of Hong Kong
nanguan@cityu.edu.hk

Kui Wu
University of Victoria
wkui@uvic.ca

Yung-Hui Li
Hon Hai Research Institute
yunghui.li@foxconn.com

Yu-Kai Huang
Carnegie Mellon University
yukaih2@andrew.cmu.edu

Chun Jason Xue
Mohamed bin Zayed University of Artificial Intelligence
jason.xue@mbzuai.ac.ae

Abstract

Simulating realistic interactions among traffic agents is crucial for efficiently validating the safety of autonomous driving systems. Existing leading simulators primarily use an encoder-decoder structure to encode the historical trajectories for future simulation. However, such a paradigm complicates the model architecture, and the manual separation of history and future trajectories leads to low data utilization. To address these challenges, we propose Behavior Generative Pre-trained Transformers (BehaviorGPT), a decoder-only, autoregressive architecture designed to simulate the sequential motion of multiple agents. Crucially, our approach discards the traditional separation between "history" and "future," treating each time step as the "current" one, resulting in a simpler, more parameter- and data-efficient design that scales seamlessly with data and computation. Additionally, we introduce the Next-Patch Prediction Paradigm (NP3), which enables models to reason at the patch level of trajectories and capture long-range spatial-temporal interactions. BehaviorGPT ranks first across several metrics on the Waymo Sim Agents Benchmark, demonstrating its exceptional performance in multi-agent and agent-map interactions. We outperformed state-of-the-art models with a realism score of 0.741 and improved the minADE metric to 1.540, with an approximately 91.6% reduction in model parameters.

Keywords: Multi-Agent Systems, Transformers, Decoder-Only Architecture, Autonomous Driving

1 Introduction

Autonomous driving has emerged as an unstoppable trend, with its rapid development increasing the demand for faithful evaluation of autonomy systems' reliability [30]. While on-road testing can

---

[*]Equal contribution

measure driving performance by allowing autonomous vehicles (AVs) to interact with the physical world directly, the high cost per test and the scarcity of safety-critical scenarios in the real world have hindered large-scale and comprehensive evaluation. As an alternative, validating system safety via simulation has become increasingly attractive [15, 46, 50, 42] as it enables rapid testing in diverse driving scenarios simulated at a low cost. This work focuses on smart agent simulation, i.e., simulating the behavior of traffic participants such as vehicles, pedestrians, and cyclists in the digital world, which is critical for efficiently validating and iterating behavioral policies for AVs.

A good simulator should be realistic, matching the real-world distribution of multi-agent behaviors to support the assessment of AVs' ability to coexist with humans safely. To this end, researchers started by designing naive simulators, which mainly replay the driving logs collected in the real world [27, 29]. When testing new driving policies that deviate from the ones during data collection, agents in such simulators often exhibit unrealistic interactions with AVs, owing to the lack of reactivity to AVs' behavior changes. To simulate reactive agents, traditional approaches [15, 28] apply traffic rules to control agents heuristically [43, 26], which may struggle to capture real-world complexity. Recently, the availability of large-scale driving data [6, 16, 48], the emergence of powerful deep learning tools [19, 45, 20], and the prosperity of related fields such as motion forecasting [17, 44, 54, 40, 53], have spurred the development of learning-based agent simulation [42, 4, 24, 49, 52] towards more precise matching of behavioral distribution. With the establishment of standard benchmarks like the Waymo Open Sim Agents Challenge (WOSAC) [30], which systematically evaluates the realism of agent simulation in terms of kinematics, map compliance, and multi-agent interaction, the research on data-driven simulation approaches has been further advanced [47, 33].

Existing learning-based agent simulators [42, 4, 24, 49, 52, 47, 33] mainly mirror the techniques from motion forecasting [17, 44, 54, 40, 53, 39, 18] and opt for an encoder-decoder architecture, presumably due to the similarity between the two fields. Typically, these models use an encoder to extract historical information and a decoder to predict agents' future states leveraging the encoded features. This paradigm requires manually splitting the multi-agent time series into a history and a future segment, with the two segments being processed by separate encoders and decoders with heterogeneous architecture. For example, MVTA [47] constructs training samples by randomly selecting a "current" timestamp to divide sequences into history and future components. Others [49, 33] use fixed-length agent trajectories as historical scene context, conditioned on which the multi-agent future is sampled from the decoder. Nonetheless, the benefit of spending a large part of model parameters and computing budget on historical scene encoding is unclear. Using heterogeneous encoding and decoding modules also complicates the architecture, which may harm the scalability of models. Moreover, the manual separation of history and future leads to low utilization of data and computation: as every point in the sequence can be used for the separation, we believe a sample-efficient framework should be able to learn from every possible history-future pair from the sequence in parallel, which cannot be easily achieved by encoder-decoder solutions.

Inspired by the success of Large Language Models (LLMs) [35, 36, 5], we introduce the first decoder-only autoregressive architecture, termed Behavior Generative Pre-trained Transformers (BehaviorGPT), into the field of smart agent simulation to overcome the limitation of previous works. By applying homogeneous Transformer blocks [45] to the complete trajectory snippets without differentiating history and future, we arrive at a simpler, more parameter-efficient, and more sample-efficient behavior simulator with greater potential to scale up. Utilizing relative spacetime representations [53], BehaviorGPT symmetrically models each agent state in the sequence as if it were the "current" one and tasks each state with modeling subsequent states' distribution during training. As a result, our framework maximizes the utilization of agent data for autoregressive modeling, avoiding wasting any learning signals available in the time series.

Autoregressive modeling with imitation learning, however, suffers from compounding errors [37] and causal confusion [12]. For the behavior simulation task, we observed that blindly mimicking LLMs' training paradigm of next-token prediction [33], regardless of the difference in tokens' semantics across tasks, will make these issues more prominent. For a next-token prediction model where each token embeds an agent state in 0.1 seconds, achieving a low training loss can be simply copying and pasting the current token as the next one without performing any long-range interaction reasoning in space or time. To mitigate this problem, we introduce a Next-Patch Prediction Paradigm (NP3) that enables models to reason at the patch level of trajectories, as illustrated in Fig. 1. By enforcing models to autoregressively generate the next trajectory patch containing multiple time steps, which requires understanding the high-level semantics of agent behavior and capturing long-range spatial-

temporal interaction, we prevent models from leveraging simple shortcuts during training. We equip BehaviorGPT with NP3 and attain superior performance on WOSAC [30] with merely 3M model parameters, demonstrating the effectiveness of our modeling framework for smart agent simulation.

The main contributions of this paper are as follows:

- Proposed the first decoder-only autoregressive architecture for smart agent simulation, which consists of homogeneous Transformer blocks that can process complete agent sequences with high parameter and sample efficiency;
- Developed the Next-Patch Prediction scheme to enhance models' capability of long-range interaction reasoning, leading to more realistic multi-agent simulation over a long horizon;
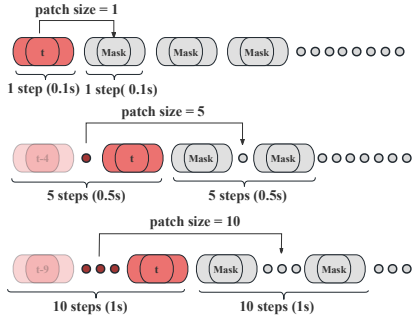- Achieved the top-ranking result in the Waymo Open Sim Agents Challenge.

Figure 1: **Next-Patch Prediction Paradigm** with patch sizes of 1, 5, and 10 time steps for trajectories sampled at 10 Hz. The capsules in dark red represent the agent states at the current time step t, while the faded red capsules indicate the agent's past states. The grey circles represent the masked agent states required for prediction.

2 Related Work

2.1 Multi-Agent Traffic Simulation

Multi-agent traffic simulation is crucial for developing and testing autonomous driving systems. From early systems like ALVINN [34] to contemporary simulators such as CARLA [15] and SUMO [28], these platforms use heuristic driving policies to simulate agent reactive behaviors [8, 7, 11]. Recent innovations include realistic simulators like Nocturne and the integration of learned sim agents that employ complex dynamics models and varied input modalities. However, these approaches struggle to capture real-world complexity as policies based on simple heuristics are not robust enough to handle all possible scenarios and need frequent updates when encountering unsolvable situations. With the availability of large-scale data and deep learning approaches, the use of generative models like VAEs [42], GANs [24], Diffusion [52], and Autoregressive models [47, 33] has also been observed in the modeling of multi-agent trajectories, which greatly enhances the realism and predictive capabilities of these simulations. Given the temporal dependency of agents' trajectory, Autoregressive models are naturally more suitable for this task, while other generative models require extra design to encode such dependencies. Among the existing autoregressive models, two representatives are MVTA [47] and Trajeglish [33], but their complicated scene context encoders make them have poor scalability and require more data to obtain acceptable performance. Hence, there is an urgent need to develop parameter- and sample-efficient model for multi-agent traffic simulation.

2.2 Patch in Transformer

The application of patches in Transformer models has demonstrated significant potential across various data modalities. PatchTST [32] introduces a patching mechanism that leverages channel-independence to retain local semantic information more effectively while significantly reducing computational complexity. In natural language processing, BERT [13] employs subword tokenization [38], while in computer vision, the Vision Transformer segments images into 16×16 patches [14]. This design has found similar applications in time series forecasting, aiming to retain local semantic information and reduce computational complexity. By dividing time series data into subseries-level patches, these patches serve as input tokens for the Transformer model, enabling the model to handle longer historical data and enhance forecasting accuracy. Moreover, patching has proven effective in self-supervised learning, significantly improving representation learning performance and achieving

excellent fine-tuning results on large datasets [2, 22, 3]. As trajectory prediction also deals with time series data, the patching mechanism is expected to help models better capture the complicated interaction relationships among road users and promote prediction performance.

3 Methodology

This section presents the proposed BehaviorGPT for multi-agent behavior simulation, with Fig. 2 illustrating the overall framework. To begin with, we provide the formulation of our map-conditioned, multi-agent autoregressive modeling. Then, we detail the architecture of BehaviorGPT, which adopts a Transformer decoder with a triple-attention mechanism to operate sequences at the patch level. Finally, we present the objective for model training.
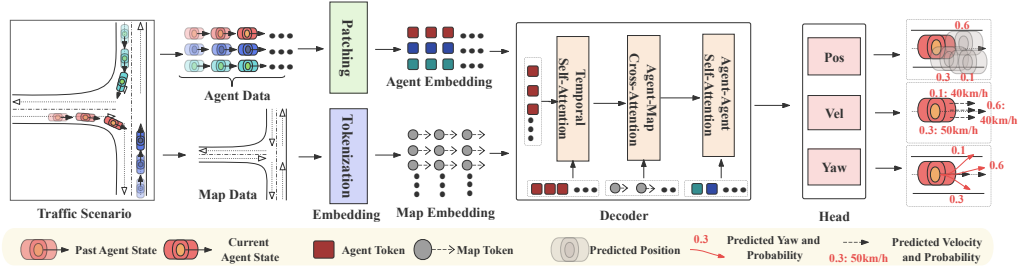

Figure 2: **Overview of BehaviorGPT.** Agent and map data are embedded and fed into a Transformer decoder for autoregressive modeling based on next-patch prediction.

3.1 Problem Formulation

In multi-agent behavior simulation, we aim to simulate agents' future behavior in dynamic and complex environments. Specifically, we define a scenario as the composite of a vector map M and the states of N_{agent} agents over T time steps. At each time step, the state of the i-th agent S_i includes the agent's position, velocity, yaw angle, and bounding box size. The semantic type of agents (e.g., vehicles, pedestrians, and cyclists) are also available. Given the sequential nature of agent trajectories, we formulate the problem as sequential predictions over trajectory patches, where the prediction of a previous patch will affect that of the next patch. We define an agent-level trajectory patch as follows:

$$P_i^\tau = S_i^{(\tau-1)\times\ell+1:\tau\times\ell} \, , \, i \in \{1, \ldots, N_{\text{agent}}\} \, , \, \tau \in \{1, \ldots, N_{\text{patch}}\} \, , \tag{1}$$

where ℓ is the number of time steps covered by a patch, $N_{\text{patch}} = T/\ell$ indicates the number of patches, and P_i^τ represents the τ-th trajectory patch of the i-th agent, with $S_i^{(\tau-1)\times\ell+1:\tau\times\ell}$ denoting the states within the patch. On top of P_i^τ, we use P^τ to denote the τ-th scene-level patch:

$$P^\tau = S_{1:N_{\text{agent}}}^{(\tau-1)\times\ell+1:\tau\times\ell} \, , \, \tau \in \{1, \ldots, N_{\text{patch}}\} \, , \tag{2}$$

where P^τ incorporates all agents' states at the τ-th patch. Next, we factorize the multi-agent joint distribution over scene-level patches according to the chain rule, following which we further factorize the distribution of each scene-level patch over the agents based on the assumption that each agent executes the plan independently within the horizon of a patch:

$$
\begin{aligned}
\Pr\left(S_{1:N_{\text{agent}}}^{1:T} \mid M\right) &= \Pr\left(P^{1:N_{\text{patch}}} \mid M\right) \\
&= \prod_{\tau=1}^{N_{\text{patch}}} \Pr\left(P^\tau \mid P^{1:\tau-1}, M\right) \\
&= \prod_{\tau=1}^{N_{\text{patch}}} \prod_{i=1}^{N_{\text{agent}}} \Pr\left(P_i^\tau \mid P^{1:\tau-1}, M\right) \, .
\end{aligned}
\tag{3}
$$

4

Here, we denote by $\Pr(S_{1:N_{\text{agent}}}^{1:T} \mid M)$ the joint distribution of all agents' states over all time steps conditioned on the map M. Considering the multimodality of agents' behavior over the horizon of a patch, we assume $\Pr(P_i^\tau \mid P^{1:\tau-1}, M)$ to be a mixture model consisting of N_{mode} modes:

$$
\begin{aligned}
\Pr\left(P_i^\tau \mid P^{1:\tau-1}, M\right) &= \sum_{k=1}^{N_{\text{mode}}} \pi_{i,k}^\tau \Pr\left(P_{i,k}^\tau \mid P^{1:\tau-1}, M\right) \\
&= \sum_{k=1}^{N_{\text{mode}}} \pi_{i,k}^\tau \Pr\left(S_{i,k}^{(\tau-1)\times\ell+1:\tau\times\ell} \mid P^{1:\tau-1}, M\right) \\
&= \sum_{k=1}^{N_{\text{mode}}} \pi_{i,k}^\tau \prod_{t=(\tau-1)\times\ell+1}^{\tau\times\ell} \Pr\left(S_{i,k}^t \mid S_{i,k}^{(\tau-1)\times\ell+1:t-1}, P^{1:\tau-1}, M\right),
\end{aligned}
\tag{4}
$$

where $\pi_{i,k}^\tau$ is the probability of the k-th mode. Given the sequential nature of the states within a patch, Eq. 4 also conducts factorization over the states per mode using the chain rule.

3.2 Relative Spacetime Representation

In our autoregressive formulation, we treat each trajectory patch as the "current" patch that is responsible for estimating the next-patch distribution during training, contrasting many existing approaches that designate one current time step per sequence [49, 47, 23]. As a result, it is inefficient to employ the well-established agent- or polyline-centric representation from the field of motion forecasting [44, 54, 31, 40, 25, 51, 41], given that these representations are computed under the reference frames determined by one current time step per sequence. For this reason, we adopt the relative spacetime representation introduced in QCNet [53] to model the patches symmetrically in time, thereby allowing parallel next-patch predictions. Under this representation, the features of each map element and agent state are derived from coordinate-independent attributes (e.g., the semantic category of a map element and the speed of an agent state). On top of this, we effectively maintain the spatial-temporal relationships between input elements via relative positional embeddings. Specifically, we use i and j to index two different input elements and compute the relative spatial-temporal embedding by:

$$
\mathcal{R}_{j\to i} = \text{MLP}\left(\|\boldsymbol{d}_{j\to i}\|, \angle\left(\boldsymbol{n}_i, \boldsymbol{d}_{j\to i}\right), \Delta\boldsymbol{\theta}_{j\to i}, \Delta\boldsymbol{\tau}_{j\to i}\right),
\tag{5}
$$

where $R_{j\to i}$ is the relational embedding from j to i, $\|d_{j\to i}\|$ is the Euclidean distance between them, $\angle(n_i, d_{j\to i})$ is the angle between n_i (the orientation of i) and $d_{j\to i}$ (the displacement vector from j to i), $\Delta\theta_{j\to i}$ is the relative yaw angle from j to i, and $\Delta\tau_{j\to i}$ is the time difference between them.

3.3 Map Tokenization and Agent Patching

Before performing spatial-temporal relational reasoning among the input elements of a traffic scenario, we must convert the raw information into high-dimensional embeddings. We first embed map information by sampling map points per 5 meters from the road graph and tokenizing them according to their semantic category (e.g., lane centerlines, road edges, and crosswalks). The i-th map point's embedding is denoted by $\hat{M}_i$. On the other hand, we process agent states using attention-based patching to obtain patch-level embeddings of trajectories. For the i-th agent's state S_i^t at time step t, we employ an MLP to transform the speed, the velocity vector's yaw angle relative to the bounding box's heading, the size of the bounding box, and the semantic type of the agent, into a feature vector $\hat{S}_i^t$. To further acquire patch embeddings, we collect the feature vectors of ℓ consecutive agent states and apply the attention mechanism with relative positional embeddings to them:

$$
\hat{P}_i^\tau = \text{MHSA}(Q = \hat{S}_i^{\tau\times\ell}, K = V = \{[\hat{S}_i^t, \mathcal{R}_i^{t\to\tau\times\ell}]\}_{t\in\{(\tau-1)\times\ell+1,\ldots,\tau\times\ell-1\}}),
\tag{6}
$$

where $\hat{P}_i^\tau$ is the patch embedding of the i-th agent at the τ-th patch, $\text{MHSA}(\cdot)$ denotes the multi-head self-attention [45], $[:, :]$ denotes concatenation, and $\mathcal{R}_i^{t\to\tau\times\ell}$ indicates the positional embedding of S_i^t relative to $S_i^{\tau\times\ell}$, which is computed according to Eq. 5. Such an operation can be viewed as aggregating the features of $S_i^{(\tau-1)\times\ell+1:\tau\times\ell-1}$ into that of $S^{\tau\times\ell}$ and using the embeddings fused with high-level semantics as the agent tokens in the subsequent modules.

3.4 Triple-Attention Transformer Decoder

After obtaining the map tokens and the patch embeddings of agents, we employ a Transformer decoder [45] with the triple-attention mechanism to model the spatial-temporal interactions among the scene elements. The triple-attention mechanism considers three distinct sources of relations in the scene: the temporal dependencies over the trajectory patches per agent, the regulations of the map elements on the agents, and the social interactions among agents, as illustrated in Figure 3.
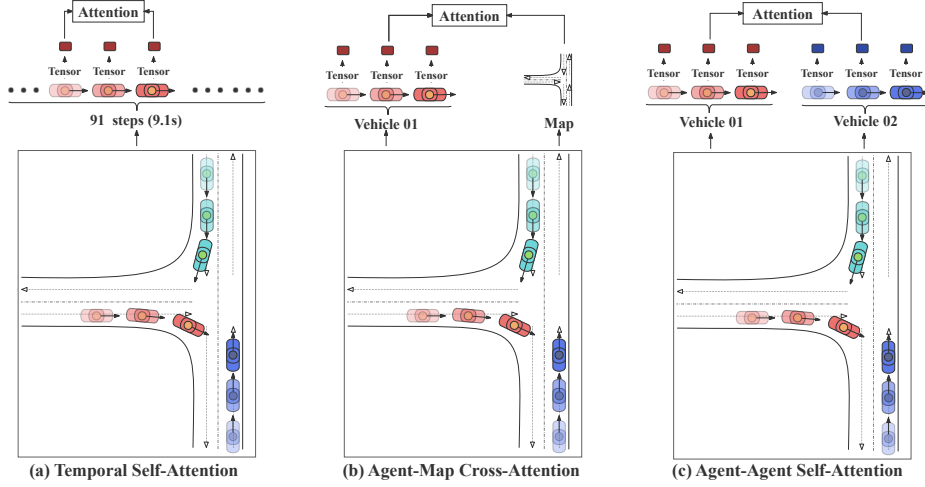

Figure 3: **Triple Attention** applies attention mechanisms to model (a) agents' individual behaviors, (b) agents' relationships with the map context, and (c) the interactions among agents.

Temporal Self-Attention. This module captures the relationships among the trajectory patches of each individual agent. Similar to decoder-only LLMs [35, 36, 5], this module leverages the multi-head self-attention (MHSA) with a causal mask to enforce each trajectory patch to only attend to its preceding patches of the same agent, which is compatible with our autoregressive formulation. We equip the temporal MHSA with relative positional embeddings, which is as shown below:

$$F_{a2t,i}^{\tau} = \text{MHSA}(Q = \hat{P}_i^{\tau}, K = V = \{[\hat{P}_i^t, \mathcal{R}_i^{t \times \ell \to \tau \times \ell}]\}_{t \in \{1,...,\tau-1\}}), \tag{7}$$

where $F_{a2t,i}^{\tau}$ and $\hat{P}_i^{\tau}$ are the temporal-aware feature vector and the patch embedding for the i-th agent at the τ-th patch, respectively, and $\mathcal{R}_i^{t \times \ell \to \tau \times \ell}$ embeds the relative position from $S_i^{t \times \ell}$ to $S_i^{\tau \times \ell}$, which represents the spatial-temporal relationship between the patches P_i^t and P_i^{τ}.

Agent-Map Cross-Attention. Unlike natural language, which only has a sequential dimension (similar to the time dimension in our task), we must also conduct spatial reasoning to consider the environmental influence on agents' behavior. To facilitate the modeling of agent-map interactions, we apply the multi-head cross-attention (MHCA) to each trajectory patch in the scenario. Considering that a scenario may comprise an explosive number of map points and that an agent would not be influenced by map elements far away, we filter the key/value map elements in MHCA using the k-nearest neighbors algorithm. The agent-map cross-attention is formulated as:

$$F_{a2m,i}^{\tau} = \text{MHCA}(Q = F_{a2t,i}^{\tau}, K = V = \{[\hat{M}_j, \mathcal{R}_{j \to i}^{\tau \times \ell}]\}_{j \in \kappa(i,\tau)}), \tag{8}$$

where $F_{a2m,i}^{\tau}$ is the map-aware feature vector for the i-th agent at the τ-th patch, $\hat{M}_j$ is the embedding of the j-th map point, $\mathcal{R}_{j \to i}^{\tau \times \ell}$ is the relative positional embedding between the agent state $S_i^{\tau \times \ell}$ and the j-th map point, and $\kappa(i,\tau)$ denotes the k-nearest map neighbors of $S_i^{\tau \times \ell}$.

Agent-Agent Self-Attention. We further capture the social interactions among agents by applying the MHSA to the space dimension of the trajectory patches. In this module, we also utilize the locality assumption induced by the k-nearest neighbor selection for better computational and memory efficiency. Specifically, the map-aware features of trajectory patches are refined by:

$$F_{a2a,i}^{\tau} = \text{MHSA}(Q = F_{a2m,i}^{\tau}, K = V = \{[F_{a2m,j}^{\tau}, \mathcal{R}_{j \to i}^{\tau \times \ell}]\}_{j \in \kappa(i,\tau)}), \tag{9}$$

where $F_{a2a,i}^{\tau}$ is the feature vector enriched with spatial interaction information among agents for the i-th agent at the τ-th patch, $\mathcal{R}_{j\to i}^{\tau\times\ell}$ contains the relative information between the i-th and the j-th agent at the τ-th patch, and $\kappa(i,\tau)$ filters the k-nearest agent neighbors of $S_i^{\tau\times\ell}$.

Overall Decoder Architecture. Each of the triple-attention modules is enhanced by commonly used components in Transformers [45], including feed-forward networks, residual connections [19], and Layer Normalization [1] in a pre-norm fashion. To enable higher-order relational reasoning, we interleave the three Transformer layers, each of which is applied twice. We denote the ultimate feature of the i-th agent at the τ-th patch as F_i^{τ}, which will serve as the input of the prediction head for next-patch prediction modeling.
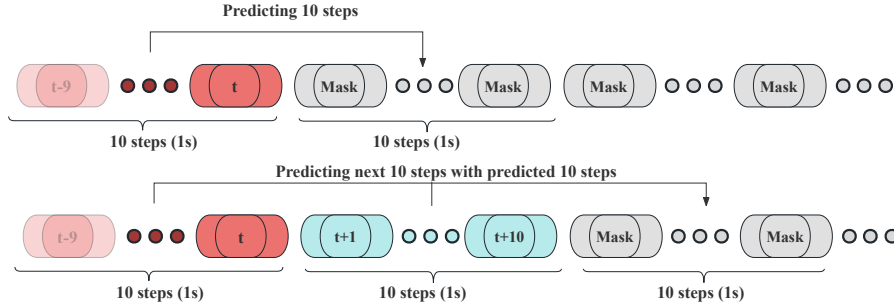
3.5 Next-Patch Prediction Head

Figure 4: **Masking Mechanism** uses the causal mask for sequential behavior simulation. The current trajectory patches represented by red capsules provide the context for predicting the subsequent steps, and the newly predicted patch (in cyan) is further utilized in the subsequent simulation steps.

Given the semantically rich and interaction-aware patch features output by the Transformer decoder, we develop a next-patch prediction head to model the multimodal distribution of agent trajectories. We employ an autoregressive masking mechanism during inference to sample agents' trajectories patch by patch. Specifically, based on the attention output of a patch, the prediction head will estimate the distribution of the next patch. After sampling the next trajectory patch from the distribution, we concatenate the predicted patch with the original sequence and continue to reason about the subsequent patches. An example with a patch size of 10 is shown in Figure 4.

The following describes the process of next-patch prediction regarding the τ-th patch of the i-th agent. Given the attention output F_i^{τ}, we intend to estimate the parameters of the next patch's mixture model, which we pre-define with N_{mode} modes. To begin with, we use an MLP to transform F_i^{τ} into $\pi_i^{\tau+1} \in \mathbb{R}^{N_{\text{mode}}}$, i.e., the mixing coefficient of the modes. On the other hand, we employ a GRU-based autoregressive RNN [10] to unroll the states within the next patch step by step, which respects the sequential nature of behavior simulation. Specifically, the hidden state $h_i^{\tau,t}$ of the RNN is initialized with F_i^{τ} and is updated by the newly predicted states step by step during the rollout. At each step of the RNN, we use an MLP to estimate the location and scale parameters of the next agent state's distribution based on the hidden state. The whole process is formulated as follows:

$$
\begin{aligned}
\pi_i^{\tau+1} &= \text{softmax}(\text{MLP}(F_i^{\tau}))\,, \\
h_i^{\tau,1} &= F_i^{\tau}\,, \\
\mu_i^{\tau\times\ell+t},\ b_i^{\tau\times\ell+t} &= \text{MLP}(h_i^{\tau,t})\,, \\
h_i^{\tau,t+1} &= \text{RNN}(h_i^{\tau,t},\ \mu_i^{\tau\times\ell+t})\,,
\end{aligned}
\tag{10}
$$

where $\{\mu_i^{\tau\times\ell+t}\}_{t\in\{1,\dots,\ell\}}$ and $\{b_i^{\tau\times\ell+t}\}_{t\in\{1,\dots,\ell\}}$ are locations and scales. We consider the distribution of the next agent state as a multivariate marginal distribution, parameterizing the position and velocity components as Laplace distributions and the yaw angle as a Von Mises distribution.

7

3.6 Training Objective

To train BehaviorGPT, we employ the negative log-likelihood loss $\mathcal{L}_{\text{NLL}}$ on the factorized $\Pr(S_{1:N_{\text{agent}}}^{1:T} \mid M)$ as formulated previously:

$$\mathcal{L}_{\text{NLL}} = \sum_{\tau=1}^{N_{\text{patch}}} \sum_{i=1}^{N_{\text{agent}}} -\log \sum_{k=1}^{N_{\text{mode}}} \pi_{i,k}^{\tau} \prod_{t=(\tau-1)\times\ell+1}^{\tau\times\ell} \Pr\left(S_{i,k}^{t} \mid S_{i,k}^{(\tau-1)\times\ell+1:t-1}, P^{1:\tau-1}, M\right). \quad (11)$$

Note that each ground-truth trajectory patch is transformed into the viewpoint of its previous patch. During training, we utilize teacher forcing to parallelize the modeling of next-patch prediction and lower the learning difficulty, but we do not use the ground-truth agent states when updating the RNN's hidden states, intending to train the model to recover from its mistakes made in next-state prediction.

4 Experiments

We use the Waymo Open Motion Dataset (WOMD) [16] to evaluate the effectiveness of our BehaviorGPT. We first introduce the dataset and the evaluation metrics, then present the rollout results obtained by BehaviorGPT on the Waymo Sim Agents Benchmark. Finally, we conduct ablation study to further compare and analyze the performance of BehaviorGPT under various settings.

4.1 Dataset and Metrics

Our experiments are conducted on the WOMD v1.2.1. The dataset comprises 486,995/44,097/44,920 training/validation/testing scenarios. Each scenario includes 11-step historical observations and 80-step future observations, totaling 9.1 seconds. We simulate up to 128 agents and generate 80 simulation steps (8 seconds) per agent at 0.1-second intervals in an autoregressive and reactive manner for evaluation. Each agent requires 32 simulations, each including x/y/z centroid coordinates and a heading value. We use 8 NVIDIA RTX 4090 GPUs to train models, where using 20% training data takes 12 hours and using 100% training data takes 2 days.

We use various metrics to evaluate our method. The minADE measures the minimum average displacement error over multiple simulated trajectories, assessing trajectory accuracy. REALISM is the meta metric that expects the simulations to match real-world observations. LINEAR ACCEL and LINEAR SPEED evaluate the realism regarding acceleration and speed. ANG ACCEL and ANG SPEED measure angular acceleration and speed used in maneuvering. DIST TO OBJ assesses the distances to objects, while COLLISION and TTC evaluate collision frequency and time to collision. Finally, DIST TO ROAD and OFFROAD measure map compliance.

4.2 Results on Waymo Sim Agents Benchmark

We evaluated the performance of our model using the Waymo Sim Agents Benchmark [30] and reported the results in Table 1. Although there were minor changes in the official calculation of metrics such as LINEAR ACCEL and COLLISION in 2024, the minADE metric remains stable and consistent. Thus, we consider minADE to be the primary metric for comparison. Our performance surpasses the state-of-the-art Trajeglish [33] across multiple metrics while also outperforming several well-established motion prediction models, including Wayformer [31], MultiPath++ [44], and MTR [40]. Notably, BehaviorGPT achieves the lowest minADE, indicating superior trajectory accuracy. Its high realism score underscores the model's ability to match the real-world distribution while also maintaining competitive performance in speed, acceleration, and collision metrics. These strengths indicate that BehaviorGPT is a robust and reliable choice for traffic agent simulation, showcasing its advanced capabilities in simulating agents' behavior in dynamic environments. As of the time we submitted the paper, the Waymo Open Sim Agents Challenge 2024 had not ended. We will update the complete results on the leaderboard in the revised version of our paper.

Besides the benchmarking results, we further compare the parameter count of BehaviorGPT against several baselines. Table 2 demonstrates that BehaviorGPT, with only 3 million parameters, achieves a notable reduction in parameter count compared with state-of-the-art models like MTR++ and MVTA. When compared against Trajeglish, BehaviorGPT achieves an approximately 91.6% reduction in parameter count. Despite its minimal parameter count, BehaviorGPT outperforms these more complex

Table 1: Results on the Leaderboard of the Waymo Open Sim Agents Challenge

Model	minADE (↓)	REALISM	LINEAR ACCEL	LINEAR SPEED	ANG ACCEL	ANG SPEED	DIST TO OBJ	COLLISION	TTC	DIST TO ROAD	OFFROAD
Random Agent [30]	50.706	0.155	0.044	0.002	0.012	0.074	0.000	0.000	0.734	0.178	0.287
Wayformer [31]	2.498	0.575	0.098	0.331	0.406	0.413	0.297	0.870	0.782	0.592	0.866
CAD [9]	2.308	0.531	0.253	0.349	0.310	0.432	0.332	0.568	0.789	0.637	0.834
MultiPath++ [44]	2.049	0.533	0.230	0.434	0.452	0.515	0.345	0.567	0.812	0.639	0.682
MVTA [47]	1.866	0.636	0.220	0.439	0.480	0.533	0.374	0.875	0.829	0.654	0.893
MTR+++ [40]	1.679	0.608	0.107	0.414	0.436	0.484	0.347	0.861	0.797	0.654	0.895
MVTE [47]	1.674	0.645	0.222	0.445	0.481	0.535	0.383	0.893	0.832	0.664	0.908
Trajeglish [33]	1.571	0.645	0.192	0.453	0.538	0.485	0.386	0.922	0.836	0.659	0.886
Waymo Baseline (2024) [30]	7.514	0.398	0.116	0.043	0.439	0.252	0.215	0.390	0.755	0.480	0.442
MVTE (2024) [47]	1.676	0.730	**0.353**	**0.359**	**0.599**	**0.497**	0.374	0.904	0.830	0.665	0.907
BehaviorGPT (Ours)	**1.540**	**0.741**	0.315	0.355	0.530	0.469	**0.377**	**0.952**	0.828	**0.666**	**0.930**

models, as shown in Table 1. These results demonstrate the parameter efficiency of decoder-only architecture and also indicate that our approach can utilize the training samples more efficiently.

Table 2: Comparison on Model Parameter

	BehaviorGPT (Ours)	Trajeglish [33]	MTR++ [41]	MTR [41]	MVTA [47]
#Parameter	3M	35.6M	86.6M	65.8M	> 65.8M

4.3 Impact of Hyperparameters

In BehaviorGPT, four model hyperparameters are expected to impact model performance: the patch size, the number of spatial neighbors, the number of modes, and the probability threshold for trajectory mode sampling. We trained and evaluated BehaviorGPT using different hyperparameters to investigate their impact on model performance in the following.

Table 3: Comparison on the Patch Size

Model Variants	minADE (↓)	REALISM	LINEAR ACCEL	ANG SPEED	DIST TO OBJ	OFFROAD
BehaviorGPT (patch size=1)	2.3752	0.6783	0.2088	0.4021	0.3201	0.8432
BehaviorGPT (patch size=5)	1.5598	0.7272	0.3217	0.4622	0.3768	0.9077
BehaviorGPT (patch size=10)	1.5203	0.7334	0.3022	0.4733	0.3796	0.9131

Table 3 presents the results of BehaviorGPT with varying patch sizes. By comparing the 6 most representative metrics, it is evident that using a patch size of 5, meaning training and predicting with 5 steps (0.5 seconds), significantly outperforms the model without patching. Additionally, increasing the patch size to 10 further enhances the performance, though the improvement is less substantial. These results demonstrate the benefits of incorporating the NP3 into agent simulation.

The next hyperparameter to be investigated is the number of spatial neighbors considered in Transformers. Table 4 shows that increasing the neighbor number from 16 to 32 can improve the performance on all metrics, which shows that our model can easily scale up with more computation.

Lastly, the number of modes refers to the number of predicted futures in multi-modal distributions, where a larger number of modes may enhance the trajectory diversity. We also adopt top-p sampling [21] to select the smallest set of most probable tokens whose cumulative probability exceeds p, where a larger p encourages more diverse outputs. Table 5 reveals that for the same top-p value, increasing the number of modes (N_{mode}) generally improves the realism and offroad metrics but has varied effects on other metrics. For the same N_{mode}, increasing p achieves better realism and linear acceleration but slightly decreases minADE and other metrics.

5 Conclusion

In this work, we introduced BehaviorGPT, a decoder-only autoregressive architecture designed to enhance smart agent simulation for autonomous driving. By applying homogeneous Transformer blocks to entire trajectory snippets and utilizing relative spacetime representations, BehaviorGPT simplifies the modeling process and maximizes data utilization. To enable high-level understanding and long-range interaction reasoning in space and time, we developed the Next-Patch Prediction

Table 4: Model Comparison with Different Numbers of Neighbors in Spatial Attention

Model Variants	minADE ($\downarrow$)	REALISM	LINEAR ACCEL	ANG SPEED	DIST TO OBJ	OFFROAD
BehaviorGPT (k=16)	1.6463	0.7207	0.2659	0.4510	0.6540	0.8926
BehaviorGPT (k=32)	1.5930	0.7283	0.2691	0.4556	0.6550	0.9137

Table 5: Comparison on the Number of Modes and the Top-p Hyperparameter

Model Variants	minADE ($\downarrow$)	REALISM	LINEAR ACCEL	ANG SPEED	DIST TO OBJ	OFFROAD
BehaviorGPT (N_{mode}=8, p=0.95)	1.6132	0.7290	0.2630	0.4564	0.6520	0.9174
BehaviorGPT (N_{mode}=16, p=0.8)	1.6278	0.7274	0.2652	0.4557	0.6547	0.9148
BehaviorGPT (N_{mode}=16, p=0.9)	1.5671	0.7298	0.2791	0.4631	0.6606	0.9147
BehaviorGPT (N_{mode}=16, p=0.95)	1.5479	0.7310	0.2883	0.4686	0.6625	0.9131
BehaviorGPT (N_{mode}=16, p=1.0)	1.5276	0.7335	0.2959	0.4744	0.6630	0.9142

Paradigm, which requires the model to predict patches of trajectories instead of short segments. Our results on the Waymo Open Sim Agents Challenge demonstrate that BehaviorGPT, with just 3 million parameters, achieves superior performance, highlighting its potential to improve the realism and scalability of autonomous vehicle simulations with significantly fewer parameters.

References

[1] Jimmy Lei Ba, Jamie Ryan Kiros, and Geoffrey E Hinton. Layer normalization. *arXiv preprint arXiv:1607.06450*, 2016.

[2] Alexei Baevski, Yuhao Zhou, Abdelrahman Mohamed, and Michael Auli. wav2vec 2.0: A framework for self-supervised learning of speech representations. In *Advances in Neural Information Processing Systems*, volume 33, pages 12449–12460, 2020.

[3] Hangbo Bao, Li Dong, Songhao Piao, and Furu Wei. Beit: Bert pre-training of image trans-formers. *arXiv preprint arXiv:2106.08254*, 2021.

[4] Luca Bergamini, Yawei Ye, Oliver Scheel, Long Chen, Chih Hu, Luca Del Pero, Błażej Osiński, Hugo Grimmett, and Peter Ondruska. Simnet: Learning reactive self-driving simulations from real-world observations. In *2021 IEEE International Conference on Robotics and Automation (ICRA)*, pages 5119–5125. IEEE, 2021.

[5] Tom Brown, Benjamin Mann, Nick Ryder, Melanie Subbiah, Jared D Kaplan, Prafulla Dhariwal, Arvind Neelakantan, Pranav Shyam, Girish Sastry, Amanda Askell, et al. Language models are few-shot learners. In *Advances in Neural Information Processing Systems*, volume 33, pages 1877–1901, 2020.

[6] Ming-Fang Chang, John Lambert, Patsorn Sangkloy, Jagjeet Singh, Slawomir Bak, Andrew Hartnett, De Wang, Peter Carr, Simon Lucey, Deva Ramanan, et al. Argoverse: 3d tracking and forecasting with rich maps. In *Proceedings of the IEEE/CVF Conference on Computer Vision and Pattern Recognition*, pages 8748–8757, 2019.

[7] Dian Chen, Vladlen Koltun, and Philipp Krähenbühl. Learning to drive from a world on rails. In *Proceedings of the IEEE/CVF International Conference on Computer Vision*, pages 15590–15599, 2021.

[8] Dian Chen, Brady Zhou, Vladlen Koltun, and Philipp Krähenbühl. Learning by cheating. In *Conference on Robot Learning*, pages 66–75. PMLR, 2020.

[9] Hsu-kuang Chiu and Stephen F Smith. Collision avoidance detour for multi-agent trajectory forecasting. *arXiv preprint arXiv:2306.11638*, 2023.

[10] Kyunghyun Cho, Bart Van Merriënboer, Caglar Gulcehre, Dzmitry Bahdanau, Fethi Bougares, Holger Schwenk, and Yoshua Bengio. Learning phrase representations using rnn encoder-decoder for statistical machine translation. *arXiv preprint arXiv:1406.1078*, 2014.

[11] Felipe Codevilla, Matthias Müller, Antonio López, Vladlen Koltun, and Alexey Dosovitskiy. End-to-end driving via conditional imitation learning. In *2018 IEEE International Conference on Robotics and Automation (ICRA)*, pages 4693–4700. IEEE, 2018.

[12] Pim De Haan, Dinesh Jayaraman, and Sergey Levine. Causal confusion in imitation learning. *Advances in Neural Information Processing Systems*, 32, 2019.

[13] Jacob Devlin, Ming-Wei Chang, Kenton Lee, and Kristina Toutanova. Bert: Pre-training of deep bidirectional transformers for language understanding. *arXiv preprint arXiv:1810.04805*, 2018.

[14] Alexey Dosovitskiy, Lucas Beyer, Alexander Kolesnikov, Dirk Weissenborn, Xiaohua Zhai, Thomas Unterthiner, Mostafa Dehghani, Matthias Minderer, Georg Heigold, Sylvain Gelly, et al. An image is worth 16x16 words: Transformers for image recognition at scale. *arXiv preprint arXiv:2010.11929*, 2020.

[15] Alexey Dosovitskiy, German Ros, Felipe Codevilla, Antonio Lopez, and Vladlen Koltun. Carla: An open urban driving simulator. In *Conference on Robot Learning*, pages 1–16. PMLR, 2017.

[16] Scott Ettinger, Shuyang Cheng, Benjamin Caine, Chenxi Liu, Hang Zhao, Sabeek Pradhan, Yuning Chai, Ben Sapp, Charles R Qi, Yin Zhou, et al. Large scale interactive motion forecasting for autonomous driving: The waymo open motion dataset. In *Proceedings of the IEEE/CVF International Conference on Computer Vision*, pages 9710–9719, 2021.

[17] Jiyang Gao, Chen Sun, Hang Zhao, Yi Shen, Dragomir Anguelov, Congcong Li, and Cordelia Schmid. Vectornet: Encoding hd maps and agent dynamics from vectorized representation. In *Proceedings of the IEEE/CVF Conference on Computer Vision and Pattern Recognition*, pages 11525–11533, 2020.

[18] Junru Gu, Qiao Sun, and Hang Zhao. Densetnt: Waymo open dataset motion prediction challenge 1st place solution. *arXiv preprint arXiv:2106.14160*, 2021.

[19] Kaiming He, Xiangyu Zhang, Shaoqing Ren, and Jian Sun. Deep residual learning for image recognition. In *Proceedings of the IEEE Conference on Computer Vision and Pattern Recognition*, pages 770–778, 2016.

[20] Jonathan Ho, Ajay Jain, and Pieter Abbeel. Denoising diffusion probabilistic models. In *Advances in Neural Information Processing Systems*, volume 33, pages 6840–6851, 2020.

[21] Ari Holtzman, Jan Buys, Li Du, Maxwell Forbes, and Yejin Choi. The curious case of neural text degeneration. *arXiv preprint arXiv:1904.09751*, 2019.

[22] Wei-Ning Hsu, Benjamin Bolte, Yao-Hung Hubert Tsai, Kushal Lakhotia, Ruslan Salakhutdinov, and Abdelrahman Mohamed. Hubert: Self-supervised speech representation learning by masked prediction of hidden units. *IEEE/ACM Transactions on Audio, Speech, and Language Processing*, 29:3451–3460, 2021.

[23] Zhiyu Huang, Zixu Zhang, Ameya Vaidya, Yuxiao Chen, Chen Lv, and Jaime Fernández Fisac. Versatile scene-consistent traffic scenario generation as optimization with diffusion. *arXiv preprint arXiv:2404.02524*, 2024.

[24] Maximilian Igl, Daewoo Kim, Alex Kuefler, Paul Mougin, Punit Shah, Kyriacos Shiarlis, Dragomir Anguelov, Mark Palatucci, Brandyn White, and Shimon Whiteson. Symphony: Learning realistic and diverse agents for autonomous driving simulation. In *2022 International Conference on Robotics and Automation (ICRA)*, pages 2445–2451. IEEE, 2022.

[25] Xiaosong Jia, Penghao Wu, Li Chen, Yu Liu, Hongyang Li, and Junchi Yan. Hdgt: Heterogeneous driving graph transformer for multi-agent trajectory prediction via scene encoding. *IEEE transactions on pattern analysis and machine intelligence*, 2023.

[26] Arne Kesting, Martin Treiber, and Dirk Helbing. General lane-changing model mobil for car-following models. *Transportation Research Record*, 1999(1):86–94, 2007.

[27] Parth Kothari, Christian Perone, Luca Bergamini, Alexandre Alahi, and Peter Ondruska. Drivergym: Democratising reinforcement learning for autonomous driving. *arXiv preprint arXiv:2111.06889*, 2021.

[28] Daniel Krajzewicz, Georg Hertkorn, Christian Rössel, and Peter Wagner. Sumo (simulation of urban mobility)-an open-source traffic simulation. In *Proceedings of the 4th middle East Symposium on Simulation and Modelling (MESM20002)*, pages 183–187, 2002.

[29] Quanyi Li, Zhenghao Peng, Lan Feng, Qihang Zhang, Zhenghai Xue, and Bolei Zhou. Metadrive: Composing diverse driving scenarios for generalizable reinforcement learning. *IEEE Transactions on Pattern Analysis and Machine Intelligence*, 45(3):3461–3475, 2022.

[30] Nico Montali, John Lambert, Paul Mougin, Alex Kuefler, Nicholas Rhinehart, Michelle Li, Cole Gulino, Tristan Emrich, Zoey Yang, Shimon Whiteson, et al. The waymo open sim agents challenge. In *Advances in Neural Information Processing Systems*, volume 36, 2024.

[31] Nigamaa Nayakanti, Rami Al-Rfou, Aurick Zhou, Kratarth Goel, Khaled S Refaat, and Benjamin Sapp. Wayformer: Motion forecasting via simple & efficient attention networks. In *2023 IEEE International Conference on Robotics and Automation (ICRA)*, pages 2980–2987. IEEE, 2023.

[32] Yuqi Nie, Nam H Nguyen, Phanwadee Sinthong, and Jayant Kalagnanam. A time series is worth 64 words: Long-term forecasting with transformers. *arXiv preprint arXiv:2211.14730*, 2022.

[33] Jonah Philion, Xue Bin Peng, and Sanja Fidler. Trajeglish: Traffic modeling as next-token prediction. In *The Twelfth International Conference on Learning Representations*, 2024.

[34] Dean A Pomerleau. Alvinn: An autonomous land vehicle in a neural network. In *Advances in Neural Information Processing Systems*, volume 1, 1988.

[35] Alec Radford, Karthik Narasimhan, Tim Salimans, Ilya Sutskever, et al. Improving language understanding by generative pre-training. *OpenAI blog*, 2018.

[36] Alec Radford, Jeffrey Wu, Rewon Child, David Luan, Dario Amodei, Ilya Sutskever, et al. Language models are unsupervised multitask learners. *OpenAI blog*, 2019.

[37] Stéphane Ross, Geoffrey Gordon, and Drew Bagnell. A reduction of imitation learning and structured prediction to no-regret online learning. In *Proceedings of the Fourteenth International Conference on Artificial Intelligence and Statistics*, pages 627–635, 2011.

[38] Mike Schuster and Kaisuke Nakajima. Japanese and korean voice search. In *2012 IEEE international conference on acoustics, speech and signal processing (ICASSP)*, pages 5149–5152. IEEE, 2012.

[39] Ari Seff, Brian Cera, Dian Chen, Mason Ng, Aurick Zhou, Nigamaa Nayakanti, Khaled S Refaat, Rami Al-Rfou, and Benjamin Sapp. Motionlm: Multi-agent motion forecasting as language modeling. In *Proceedings of the IEEE/CVF International Conference on Computer Vision*, pages 8579–8590, 2023.

[40] Shaoshuai Shi, Li Jiang, Dengxin Dai, and Bernt Schiele. Motion transformer with global intention localization and local movement refinement. In *Advances in Neural Information Processing Systems*, volume 35, pages 6531–6543, 2022.

[41] Shaoshuai Shi, Li Jiang, Dengxin Dai, and Bernt Schiele. Mtr++: Multi-agent motion prediction with symmetric scene modeling and guided intention querying. *IEEE Transactions on Pattern Analysis and Machine Intelligence*, 2024.

[42] Simon Suo, Sebastian Regalado, Sergio Casas, and Raquel Urtasun. Trafficsim: Learning to simulate realistic multi-agent behaviors. In *Proceedings of the IEEE/CVF Conference on Computer Vision and Pattern Recognition*, pages 10400–10409, 2021.

[43] Martin Treiber, Ansgar Hennecke, and Dirk Helbing. Congested traffic states in empirical observations and microscopic simulations. *Physical Review E*, 62(2):1805, 2000.

[44] Balakrishnan Varadarajan, Ahmed Hefny, Avikalp Srivastava, Khaled S Refaat, Nigamaa Nayakanti, Andre Cornman, Kan Chen, Bertrand Douillard, Chi Pang Lam, Dragomir Anguelov, et al. Multipath++: Efficient information fusion and trajectory aggregation for behavior prediction. In *2022 International Conference on Robotics and Automation (ICRA)*, pages 7814–7821. IEEE, 2022.

[45] Ashish Vaswani, Noam Shazeer, Niki Parmar, Jakob Uszkoreit, Llion Jones, Aidan N Gomez, Łukasz Kaiser, and Illia Polosukhin. Attention is all you need. In *Advances in Neural Information Processing Systems*, volume 30, 2017.

[46] Eugene Vinitsky, Nathan Lichtlé, Xiaomeng Yang, Brandon Amos, and Jakob Foerster. Nocturne: a scalable driving benchmark for bringing multi-agent learning one step closer to the real world. In *Advances in Neural Information Processing Systems*, volume 35, pages 3962–3974, 2022.

[47] Yu Wang, Tiebiao Zhao, and Fan Yi. Multiverse transformer: 1st place solution for waymo open sim agents challenge 2023. *arXiv preprint arXiv:2306.11868*, 2023.

[48] Benjamin Wilson, William Qi, Tanmay Agarwal, John Lambert, Jagjeet Singh, Siddhesh Khandelwal, Bowen Pan, Ratnesh Kumar, Andrew Hartnett, Jhony Kaesemodel Pontes, et al. Argoverse 2: Next generation datasets for self-driving perception and forecasting. *arXiv preprint arXiv:2301.00493*, 2023.

[49] Danfei Xu, Yuxiao Chen, Boris Ivanovic, and Marco Pavone. Bits: Bi-level imitation for traffic simulation. In *2023 IEEE International Conference on Robotics and Automation (ICRA)*, pages 2929–2936. IEEE, 2023.

[50] Ze Yang, Yun Chen, Jingkang Wang, Sivabalan Manivasagam, Wei-Chiu Ma, Anqi Joyce Yang, and Raquel Urtasun. Unisim: A neural closed-loop sensor simulator. In *Proceedings of the IEEE/CVF Conference on Computer Vision and Pattern Recognition*, pages 1389–1399, 2023.

[51] Zhejun Zhang, Alexander Liniger, Christos Sakaridis, Fisher Yu, and Luc V Gool. Real-time motion prediction via heterogeneous polyline transformer with relative pose encoding. In *Advances in Neural Information Processing Systems*, volume 36, 2024.

[52] Ziyuan Zhong, Davis Rempe, Danfei Xu, Yuxiao Chen, Sushant Veer, Tong Che, Baishakhi Ray, and Marco Pavone. Guided conditional diffusion for controllable traffic simulation. In *2023 IEEE International Conference on Robotics and Automation (ICRA)*, pages 3560–3566. IEEE, 2023.

[53] Zikang Zhou, Jianping Wang, Yung-Hui Li, and Yu-Kai Huang. Query-centric trajectory prediction. In *Proceedings of the IEEE/CVF Conference on Computer Vision and Pattern Recognition*, pages 17863–17873, 2023.

[54] Zikang Zhou, Luyao Ye, Jianping Wang, Kui Wu, and Kejie Lu. Hivt: Hierarchical vector transformer for multi-agent motion prediction. In *Proceedings of the IEEE/CVF Conference on Computer Vision and Pattern Recognition*, pages 8823–8833, 2022.